

Supplementary Information

**Self-seeded growth of nest-like hydrated tungsten trioxide
film film directly on FTO substrate for highly enhanced
electrochromic performance**

Haizeng Li,^a Guoying Shi,^c Hongzhi Wang,^{*a} Qinghong Zhang^b and Yaogang Li^{*b}

^a State Key Laboratory for Modification of Chemical Fibers and Polymer Materials, College of Materials Science and Engineering, Donghua University, Shanghai 201620, P. R. China. E-mail: wanghz@dhu.edu.cn; Fax: +86-021-67792855; Tel: +86-021-67792881

^b Engineering Research Center of Advanced Glasses Manufacturing Technology, Ministry of Education, College of Materials Science and Engineering, Donghua University, Shanghai 201620, P. R. China. E-mail: yaogang_li@dhu.edu.cn; Fax: +86-021-67792855; Tel: +86-021-67792526

^c College of Chemistry, Chemical Engineering and Biotechnology, Donghua University, Shanghai 201620, China

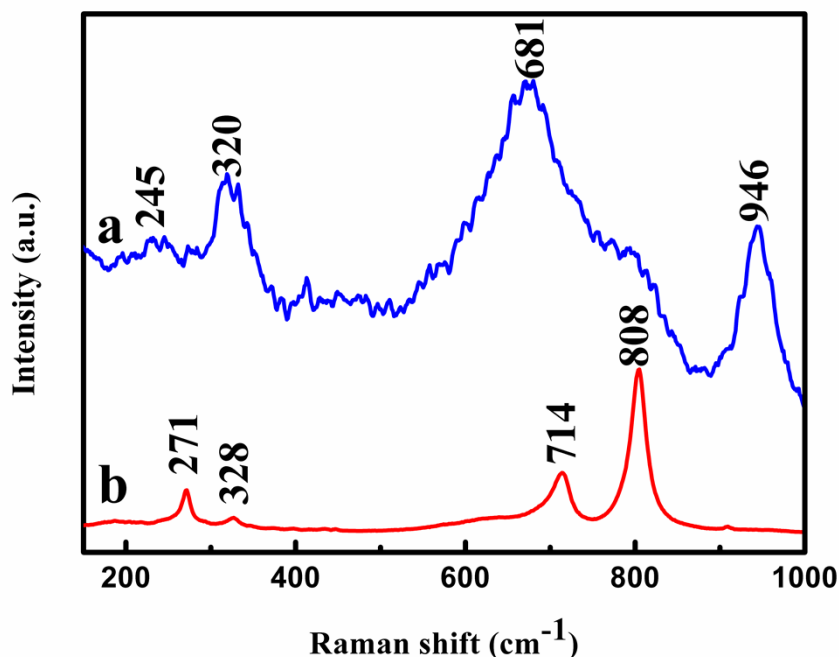


Fig. S1 Raman spectra of the films: (a) as-prepared and (b) annealed at 500 °C for 2 h.

Fig. S1 displays the Raman spectra of the as-prepared $\text{WO}_3 \cdot 0.33\text{H}_2\text{O}$ film and annealed film. The band at 681 cm^{-1} arises from the O-W-O stretching vibrations of the bridging oxygen atoms, the band at 245 cm^{-1} belongs to W-O-W bending mode and the bands at 320 cm^{-1} and 946 cm^{-1} can be assigned to the stretching of W-(OH)₂ and W=O, respectively. These vibrations are commonly found in tungsten trioxide hydrates ($\text{WO}_3 \cdot n\text{H}_2\text{O}$).¹⁻⁵ After annealed at 500 °C for 2h, the bands centered at 714 and 808 cm^{-1} arise from the O-W-O stretching vibrations of the bridging oxygen atoms, and the two bands located at 271 and 328 cm^{-1} belong to W-O-W bending modes. These vibrations indicate that the as-prepared $\text{WO}_3 \cdot 0.33\text{H}_2\text{O}$ film transforms into pure WO_3 after heattreatment.^{6,7}

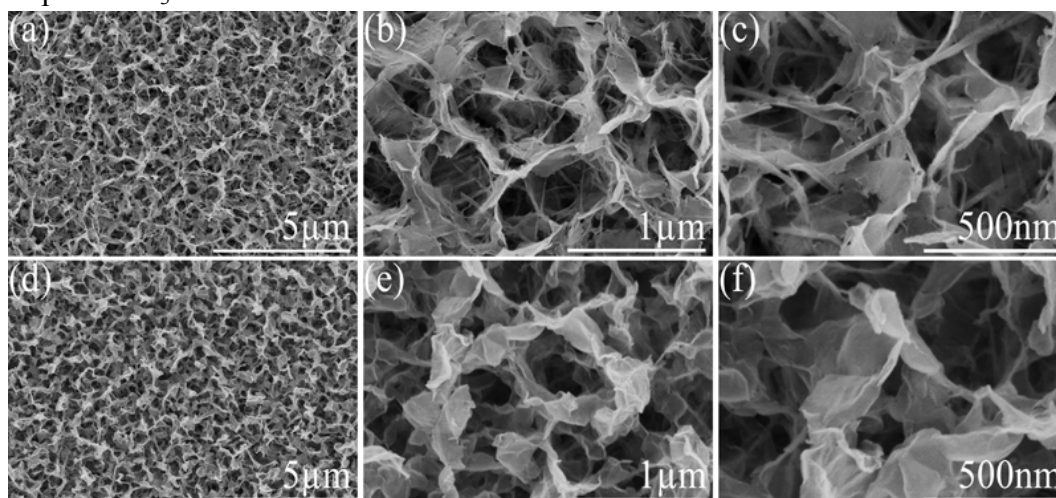


Fig. S2 FE-SEM images and corresponding high-magnification images of $\text{WO}_3 \cdot 0.33\text{H}_2\text{O}$ electrode prepared without(a,b,c) and with(d,e,f) seed layer.

Fig. S2 displays the difference of hydrothermally grown films with and without SL. The morphologies of the self-seeded grown electrode is shown in Fig. S2(a,b,c), while the morphologies of the crystal-seed-assisted grown film is shown in Fig. S2(d,e,f). The nest-like nanosheets of the self-seeded grown film are formed of nanoribbons while the nanosheets of the crystal-seed-assisted grown film are pure nanosheets. The hierarchical nanostructures create a large surface area for electrolyte to come in complete contact with the $\text{WO}_3 \cdot 0.33\text{H}_2\text{O}$ and could make the Li^+ ion intercalation and deintercalation processes easier.

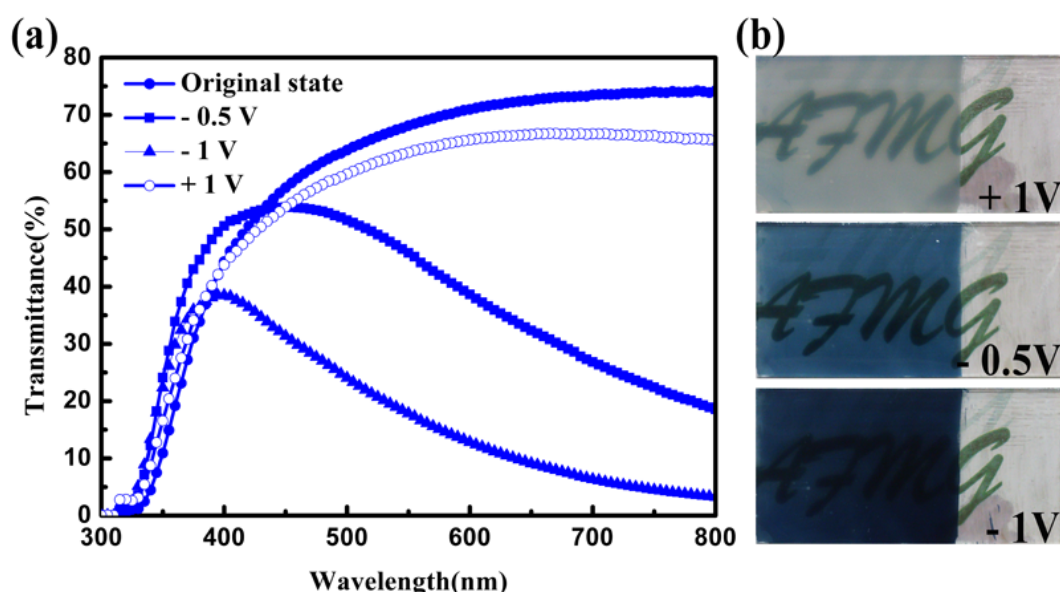


Fig. S3 (a) UV-vis transmittance spectra of the crystal-seed-assisted grown film measured at -0.5 V , -1.0 V and $+1.0\text{ V}$, respectively. (b) Digital photographs of the crystal-seed-assisted grown film.

The modulation range of the crystal-seed-assisted grown film at 632.8 nm after applying voltages of -0.5 and -1.0 V is calculated to be 32.2 and 56.2% , respectively (Fig. S3(a)), these modulation range is poor compared with that of the self-seeded grown film. Besides, the crystal-seed-assisted grown film can not recover to the original state completely after applying voltage of $+1.0\text{ V}$.

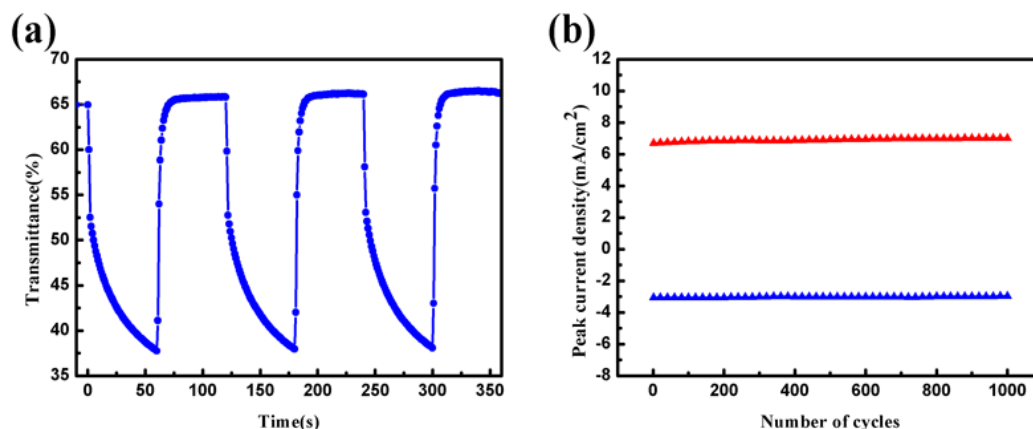


Fig. S4 (a) Switching time characteristics between the colored and bleached states for crystal-seed-assisted grown $\text{WO}_3 \cdot 0.33\text{H}_2\text{O}$ film measured at 632.8 nm , $\pm 3.0\text{ V}$ bias. (b) Peak current evolution of crystal-seed-assisted grown $\text{WO}_3 \cdot 0.33\text{H}_2\text{O}$ film during the step chronoamperometric cycles.

Fig. S4(a) shows the switching response of the crystal-seed-assisted grown film. The coloration time t_c and bleaching time t_b are calculated to be 36 s and 5.5 s respectively, while they are 26 s and 5.5 s respectively of the self-seeded grown film shown in Fig. 6(a).

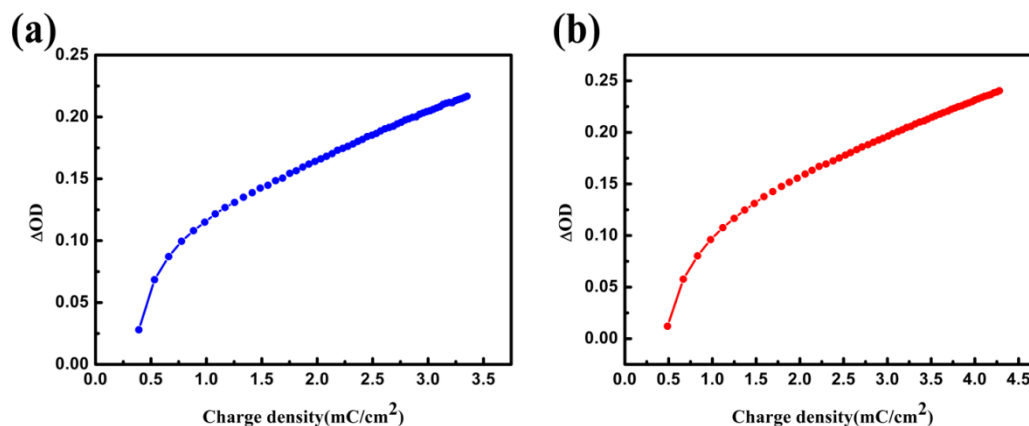


Fig. S5 OD variation with respect to the charge density for the (a) self-seeded grown $\text{WO}_3 \cdot 0.33\text{H}_2\text{O}$ film and (b) crystal-seed-assisted $\text{WO}_3 \cdot 0.33\text{H}_2\text{O}$ film measured at 632.8 nm at a potential of - 3.0 V.

Fig. S5 shows the coloration efficiency (CE) of the self-seeded grown film and crystal-seed-assisted WO_3 film. The CE values are found to be $126.34 \text{ cm}^2\text{C}^{-1}$ and $122.06 \text{ cm}^2\text{C}^{-1}$ respectively.

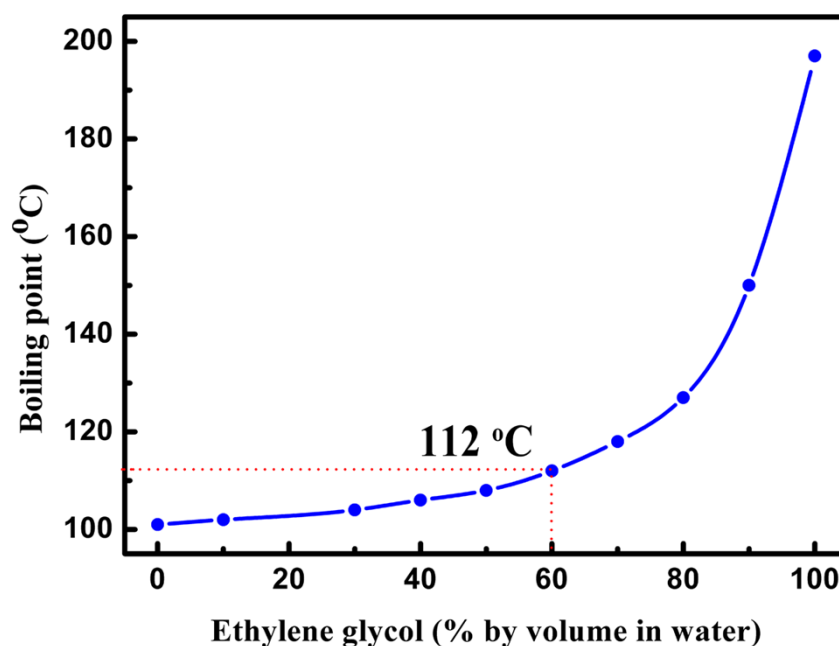


Fig. S6 Boiling point variation with respect to the composition of aqueous ethylene glycol solution

Reference:

1. K. Kalantar-zadeh, A. Vijayaraghavan, M. H. Ham, H. Zheng, M. Breedon and M. S. Strano, *Chem. Mater.*, 2010, **22**, 5660.
2. C. I. Vargas-Consuelos, K. Seo, M. Camacho-López and O. A. Graeve, *J. Phys.*

Chem. C, 2014, **118**, 9531.

3. K. Nonaka and A. Takase, *J. Mater. Sci. Lett.*, 1993, **12**, 274.

4. C. Santato, M. Odziemkowski, M. Ulmann and J. Augustynski, *J. Am. Chem. Soc.*, 2001, **123**, 10639.

5. S. Balaji, Y. Djaoued, A. S. Albert, R. Z. Ferguson and R. Brüning, *Chem. Mater.*, 2009, **21**, 1381.

6. D. Ma, H. Wang, Q. Zhang and Y. Li, *J. Mater. Chem.*, 2012, **22**, 16633.

7. X. Zhang, X. Lu, Y. Shen, J. Han, L. Yuan, L. Gong, Z. Xu, X. Bai, M. Wei, Y. Tong, Y. Gao, J. Chen, J. Zhou and Z. L. Wang, *Chem. Commun.*, 2011, **47**, 5804.